INVESTIGATION OF LIMIT EQUILIBRIUM AND FINITE ELEMENT METHODS FOR GROUND-ANCHORED SLOPES

Farnyuh Menq, Ensoft Inc., Austin, TX, USA, (512) 244-6464, f.menq@ensoftinc.com
Daqing Xu, Ensoft Inc., Austin, TX, USA, (512) 244-6464, daqing@ensoftinc.com
Luis Vasquez, Ensoft Inc., Austin, TX, USA, (512) 244-6464, gonzalo@ensoftinc.com
Shin-Tower Wang, Ensoft Inc., Austin, TX, USA, (512) 244-6464, stw@ensoftinc.com

ABSTRACT

Ground anchors are commonly used to stabilize natural slopes. The Limit Equilibrium Method (LEM) is often employed to evaluate the safety factors of the slope before and after the addition of ground anchors. However, applying a large concentrated load on the surface of the slope can cause convergence issues in the rigorous methods and cause erroneous results in simplified methods. To address these issues, Carpenter (1986) developed the Load Distribution Method. This method distributes the force throughout the potential slip surface based on Flamant's (1886) stress distribution model in a semi-infinite elastic half-space. Using the Strength Reduction Finite Element Method (SRFEM), we can evaluate the accuracy of the Load Distribution Method. A hypothetical slope with one row of ground anchors is analyzed using both LEM with the Load Distribution Method and SRFEM. Results from the modeled slope show that safety factors obtained from SRFEM are close to those obtained from LEM when a slip surface is well developed in the slope. Hence, the Load Distribution Method can provide a good approximation under those conditions. However, LEM can't model soil-structure interactions. SRFEM is needed in determining the maximum tieback force limited by a failure surface developed from soil-structure interactions.

Keywords: Limit Equilibrium Method (LEM), load distribution method, Strength Reduction Finite Element Method (SRFEM), ground anchor, tieback, slope stability

INTRODUCTION

Ground anchors (tiebacks) are commonly used for landslide stabilization and support in ground excavations. Compared to piles, constructions of ground anchors generally require smaller machines; hence, ground anchors are more cost-effective and easier to build (Lee et al., 2010). Where failure surfaces are steep, the loading demands of ground anchors are often determined from apparent earth pressure diagrams. However, loading demands of ground anchors calculated from the apparent earth pressure diagrams can underestimate the required force to stabilize a slope to reach a target Safety Factor (SF). Limit Equilibrium Method (LEM) analyses are recommended to evaluate ground anchor and wall loads for anchored slopes and landslide stabilization systems (FHWA-IF-99-015).

Applying a large concentrated tieback force on a slope surface can cause convergence issues in the rigorous slice methods (e.g., Spencer's method) and can cause erroneous results in simplified slice methods (e.g., the Simplified Bishop method). Carpenter (1985) developed the Load Distribution Method to mitigate these issues. This method distributes the force on the potential slip surface based on Flamant's (1886) stress distribution model in a semi-infinite elastic half-space. According to Flamant (1886), for a semi-infinite mass subjected to a concentrated load, P, the distribution of stresses in the radial direction can be calculated as:

$$\sigma_r = \frac{2\,P\cos(\theta)}{\pi\,R} \qquad [1]$$

where: σ_r = radial stress at a point of interest, P = concentrated load applied to an elastic half-space, R = distance to the point of interest, θ = angle formed by the line of action of the concentrated load and the line connecting the point of application of the load on the boundary surface and the point of interest. If the trial slip surface intersects the tendon portion of a row of tiebacks, the tieback force is converted into distributed normal stress on the trial failure surface, as shown in **Fig. 1**. This method is first implemented in the computer programs STABL4 and PCSTABL4 by Carpenter (Carpenter 1985 and Carpenter 2017).

Using the strength reduction algorithm, finite element analyses can provide a safety factor in slope stability analyses. The main benefit of the Strength Reduction Finite Element Method (SRFEM) for slope stability analyses is that the critical slip surface is formed naturally as soil strength reduces at each step (Griffiths and

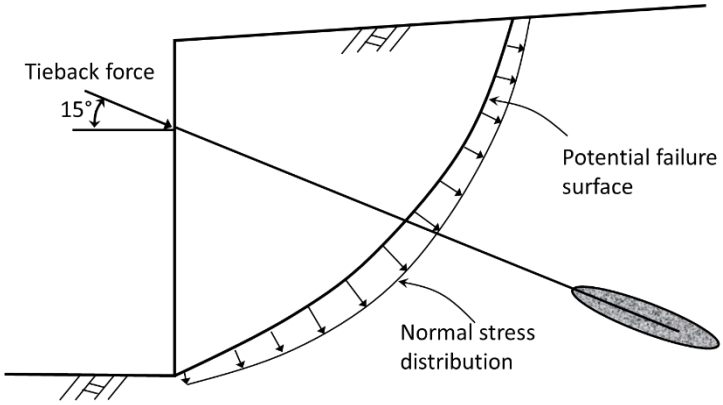

Fig. 1. Distribution of normal stress to the potential failure surface

Lane, 1999). The use of finite element analysis in routine geotechnical practice can be harder to justify, due to the significant amount of time needed to construct the model. However, there are several user-friendly SRFEM packages for slope stability analyses available in both open-source and commercial software (e.g., ABAQUS, ADONIS, EnFEM, MIDAS, OpenSees, OptumG2, Plaxis, and RS2). In addition, some Finite Element Method software provides integrated environments or import functions to facilitate SRFEM analyses from models built for LEM (e.g., MIDAS, EnFEM, and RS2). These new developments reduce the time and labor needed for SRFEM analyses.

This study utilized a commercial program, EnFEM, to examine the accuracy of the Load Distribution Method of a hypothetical slope with one row of ground anchors. Results from LEM analyses are conducted using EnSlope, formerly STABLPro, which utilizes the methodologies from Carpenter (1985 and 2017).

STRENGTH REDUCTION FINITE ELEMENT METHOD (SRFEM) FOR SLOPE STABILITY ANALYSES

Safety factors can be defined by load capacity or by strength capacity in finite element analyses. To define safety factors by load capacity, loadings (e.g., gravity, surface loads) are increased by steps until failure occurs to determine the loading capacity. Safety factors are defined as the ratio between the loading capacity and the loading demand. This is commonly used in bearing capacity analyses. On the other hand, safety factors are defined by strength capacity in slope stability analyses (Griffiths and Lane, 1999). The strengths of soils are reduced in steps until failure is reached; hence, it is named the Strength Reduction Finite Element Method (SRFEM). Safety factors, SF, in SRFEM are defined as:

$$\begin{aligned} SF &= \text{Available strength / Strength at Failure} \\ &= \tan \phi' / \tan \phi'_{mobilized} \\ &= c' / c'_{mobilized} \end{aligned} \quad [2]$$

There are two stages in an SRFEM analysis. In the first stage, loadings (e.g., gravity force, surcharges) are applied in steps to the slope. In the second stage, the strength of the soil is reduced in steps until a convergence can't be obtained. In practice, users define the range of safety factors to be analyzed. Loadings are applied to the slope with soil strength calculated from the lowest safety factor entered for the analyses. The lowest safety factor should be lower than the actual safety factor of the slope. Otherwise, a solution can't be found in the first stage, and the analysis will stop without an output of the safety factor. After completion of the first stage, the strength of the soil is reduced in steps in the second stage. Failure is defined as the algorithm cannot converge within an iteration ceiling, and/or as displacements rapidly increase in the mesh. This criterion is commonly adopted in the literature (Griffiths and Lane 1999, Griffiths and Marquez, 2007, Cheng et al., 2007, Tschuchnigg et al., 2015a & 2015b, and Theinat et al., 2024). However, the iteration ceiling and the limit of nodal displacements are not well defined. The linear elastic-perfectly plastic constitutive model with a Mohr-Coulomb failure criterion is the commonly utilized failure criterion in SRFEM. Advanced constitutive models (e.g., hardening soil, hardening soil small strain, and soft soil models) can better model soil behaviors. However, these advanced models are not available in LEM. For better comparisons between SRFEM and LEM, the Mohr-Coulomb model is used in this study.

Input parameters

The Mohr-Coulomb model is defined by six parameters. These parameters are: (1) friction angle, ϕ', (2) cohesion, c', (3) unit weight, γ, (4) Young's modulus, E, (5) Poisson's ratio, υ, and (6) dilation angle, ψ. Only the first three parameters (friction angle, cohesion, and unit weight) are required in LEM. In finite element analyses, Young's modulus and Poisson's ratio define the deformations in the linear range, and the dilation angle defines the flow rate of the soil element after yielding. Influences of the values of Young's modulus, Poisson's ratio, dilation angle, and element size on SRFEM are discussed below.

Young's modulus and Poisson's ratio

The selected Young's modulus and Poisson's ratio affect the computed deformations before failure. These two parameters have limited influence on the calculated safety factor once all elements along the slip surface have yielded. Cheng et al. (2007) investigate the influence of the soil elastic modulus with four different geometry settings. In each setting, a slope of uniform strength is separated into two regions of two different stiffnesses. The stiffness in the stiffer zone (soil 1) is assumed to be 1.4×10^5 kPa, and the stiffness in the less stiff zone (soil 2) is 1.4×10^2 kPa. The elastic moduli of soils 1 and 2 are then interchanged to determine the effect of Young's modulus. The resulting safety factors before and after the interchange of the stiffness vary by less than 2.5%. It is interesting to note that the safety factor is determined at the critical state when a slip surface has formed. All elements along the slip surface have yielded, and Young's modulus typically has minimal influence. However, as demonstrated later in this article, if tiebacks are added to the model, soil stiffness can alter the resulting tension requirements of the tiebacks. The nominal values of Young's modulus (10^5 kPa) and Poisson's ratios (0.3) suggested by Griffiths and Lane (1999) are adopted in this study.

Dilation Angle

The dilation angle (ψ) defines plastic deformations of soil elements after yielding. If the dilation angle (ψ) is equal to the friction angle (ϕ'), the flow rule is associated. If $\psi \neq \phi'$, the flow rule is non-associated. Failure mechanisms generated by finite elements with the associated flow rule are expected to be closer to critical slip surfaces predicted by LEM than those from non-associated flow rules (Griffiths and Lane, 1999, and Tschuchnigg et al., 2015a). However, the dilation angle also defines the volume changes of the yielded elements. A positive dilation angle will be accompanied by a volume increase. Similarly, a negative dilation angle will be accompanied by a volume decrease. For most soils with a friction angle greater than 0, the volume changes are much smaller than those calculated from the associated flow rule assumption. The associated volume changes can increase the strength of an element if the element is confined. Slope stability analysis is relatively unconfined, so the choice of dilation angle is less critical than that in a bearing capacity analysis; hence, Griffiths and Lane (1999) suggested using a compromised value of $\psi = 0$.

Although a smaller dilatancy angle can better model the volume change of soil elements, it can result in numerical instability with no clear indication of the failure mechanism. The solution of the governing equations is not unique for a non-associated flow rule. (Tschuchnigg et al., 2015a & 2015b, Nordal, 2008, Krabbenhoft et al., 2012). Using the Plaxis program, Tschuchnigg et al. (2015a) demonstrate the failure mechanisms of a 45° slope of a uniform soil ($\phi' = 45°$ and $c' = 6$ kPa) oscillate with increasing steps of calculation when ψ is selected to be equal to or less than 10°. This oscillation is not observed when ψ is selected to be equal to or greater than 15°. Results from Tschuchnigg et al. (2015a and 2015b) also show that oscillations do not occur if a coarser element size is used, and oscillations are more pronounced if smaller element sizes are utilized. The resulting safety factors from the associated flow rule are higher than those from the non-associated flow rule. Cheng et al. (2007) also show that safety factors from the associate flow rule are higher. **Fig. 2** shows a comparison between safety factors from these two studies. Both studies utilized the Morgenstern-Price method in LEM analyses. As shown in the figure, results from SRFEM are close to those from LEM, and safety factors from the associated flow rule ($\psi = \phi'$) are higher than those from the non-associated flow rule ($\psi = 0$).

Comparison between LEM and SRFEM is better shown as the difference between safety factors obtained from SRFEM and safety factors obtained from LEM, as shown in **Fig. 3**. The differences between the safety factors from LEM and SRFEM range from – 0.2 to + 0.2. This range is relatively wide for slope stability analyses. Comparisons from other studies, including a special case with a thin weak layer presented by Cheng et al. (2007) and results presented by Griffiths and Lane (1999) and Burman et al. (2015), are added in **Fig. 3**. The special case presented by Cheng et al. (2007) contains a thin weak layer ($\phi' = 25°$ and $c' = 0$). Due to this thin-

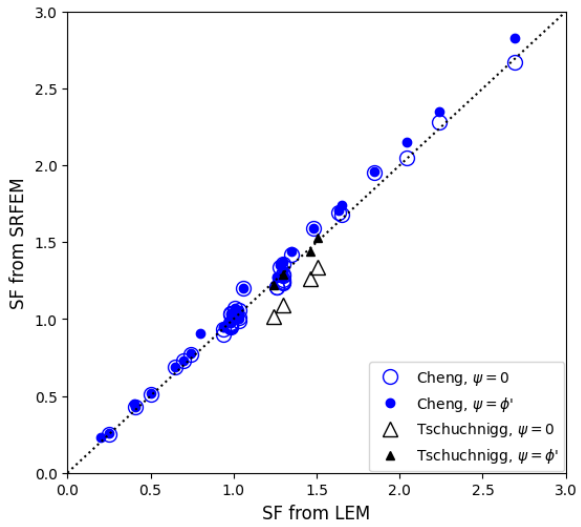

Fig. 2. SF from SRFEM vs. SF from LEM

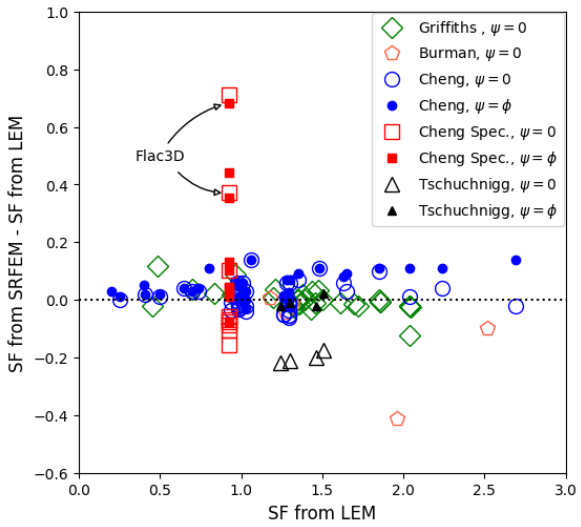

Fig. 3. Difference between SF from SRFEM and SF from LEM vs. SF from LEM

weak layer, the resulting safety factors show much more variation; hence, 3 different commercial programs are utilized by Cheng et al. (2007) to determine the factors of safety. The range of the safety factor increased in this special case to be between -0.4 and 0.8. It should be noted that in the results from Flac3D, safety factors from the associated flow rule are lower than those from the non-associated flow rule ($\psi = 0$). Cheng et al. (2007) did not discuss the cause of this reverse trend. Both Griffiths and Lane (1999) and Burman et al. (2015) only presented results for $\psi = 0$. It is interesting to note that the differences between the safety factors from LEM and SRFEM from Griffiths and Lane (1999) are smaller. This might be due to the relatively larger size elements used in their study. Overall, the differences between the safety factors from LEM and SRFEM are mostly within -0.2 and +0.2.

Element size

Ashford and Sitar (2001) show that an element height of H/10 (H: slope height) commonly used in FEM analyses of embankment slopes is adequate. However, they also indicate that an element height of H/32 is necessary to accurately determine tensile stresses within the vicinity of the slope. Theinat et al. (2004) utilize element sizes as small as 5 times the median particle size (~H/700) for soil elements in contact with the retaining wall. Tschuchnigg et al. (2015a) conducted sensitivity studies on element size and showed that an element size of H/25 provides an adequate solution. **Fig. 4** shows the results of four element sizes from a hypothetical 45° slope of a uniform soil layer modeled in this study. The color gradients shown in the figure represent the equivalent magnitude of plastic strain. Parameters of the soil layer are listed as Model A in **Table 1**. The element widths of the four element sizes are 1.0 m, 0.6 m, 0.3 m, and 0.1 m, which are approximately H/11, H/19, H/38, and H/113, respectively. The quadratic triangular element with six nodes and three straight edges (T6) available in EnFEM is utilized in this study. It should be noted that a slightly larger element size is used in regions away from the slip surface in the model with the small-size element to reduce computational time. As shown in **Fig. 4**, the slip surface is more refined using a smaller element size. The resulting safety factor reduces from 0.993 for the extra-large size elements to 0.967 for the small-size elements.

Table 1. Soil and tieback parameters utilized in SRFEM

	Tieback		Soil					
Model	Diameter (inch/cm)	Prestress (kN)	c' (kN)	ϕ' (°)	γ (kN/m^3)	E (kPa)	υ	Ψ (°)
A	None	N/A	4.79	28	19.63	1.0E+05	0.3	28
B	1.0/2.54	0	4.79	28	19.63	1.0E+05	0.3	28
C	1.0/2.54	0	4.79	28	19.63	1.0E+05	0.3	0
D	1.0/2.54	450	4.79	28	19.63	1.0E+05	0.3	28
E	1.0/2.54	0	4.79	28	19.63	1.0E+04	0.3	28
F	2.5/6.35	0	4.79	28	19.63	1.0E+05	0.3	28

The safety factors from the simplified Bishop method and Spencer's method are 0.974 and 0.969, respectively. Both the simplified Bishop method and Spencer's method yield the same critical slip surface. As shown in **Fig. 4**, the difference between the results from the regular-size elements and those from the small-size elements is negligible. The regular-size elements are used in the remainder of this study.

If the non-associated flow rule ($\psi = 0$) is used, convergence issues are encountered in all four element sizes. The safety factor from the last converged step ranges between 0.913 and 0.806 from an element size of 1 m and 0.1m, respectively. Results show no fully developed slip surface from element sizes of 0.6 m, 0.3 m, and 0.1 m at the last converged step. These safety factors from the non-associated flow rule can't be considered as the safety factor of the slope. These results illustrate the difficulty of determining the safety factor based on the last converged step.

SRFEM SLOPE STABILITY ANALYSES OF A TIEBACK SLOPE

A single row of tiebacks is added to the mid-height of the model slope in the previous example, as shown in **Fig. 5**. The tiebacks have a spacing of 10 m and a 15° inclination. The unbonded length of the tieback is 12 m with a 5 m long anchor. A relatively longer anchor length is selected to avoid pull-out failure of the tieback anchor. A 1-inch (2.54 cm) diameter steel bar with an ultimate strength of 567 kN and a 2.5-inch (6.35cm) diameter with an ultimate strength of 3,457 kN are modeled in this study. The Young's modulus of the tieback is 200 GPa. A concrete facing is added to the surface of the slope using 0.2 m thick beam elements. Young's modulus of the concrete facing is 25 GPa. Tie (fixed) connections are used between soil elements and wall elements, and between soil elements and the tieback anchor.

Five different settings of the soil and tieback parameters are modeled in this study. These 5 settings are listed as Model B to Model F in **Table 1**. In all five settings, the range of the safety factor search is set to be between 1.0 and 2.0 for the strength reduction stage of the SRFEM analyses, and soil strength at a safety factor of 1 is used in stage 1. The gravity load is applied to the soil mass in stage 1. Structure elements, including the wall, the tieback, and the tieback anchor, are activated in the first stage. However, if a prestress is applied to the tieback, a pair of point loads (representing the tension force) is applied to the endpoints of the tieback on the concrete facing and on the anchor. The tieback element is connected after stage 1 is completed. In the second stage, the strength parameters of the soil are reduced by steps until the algorithm cannot converge.

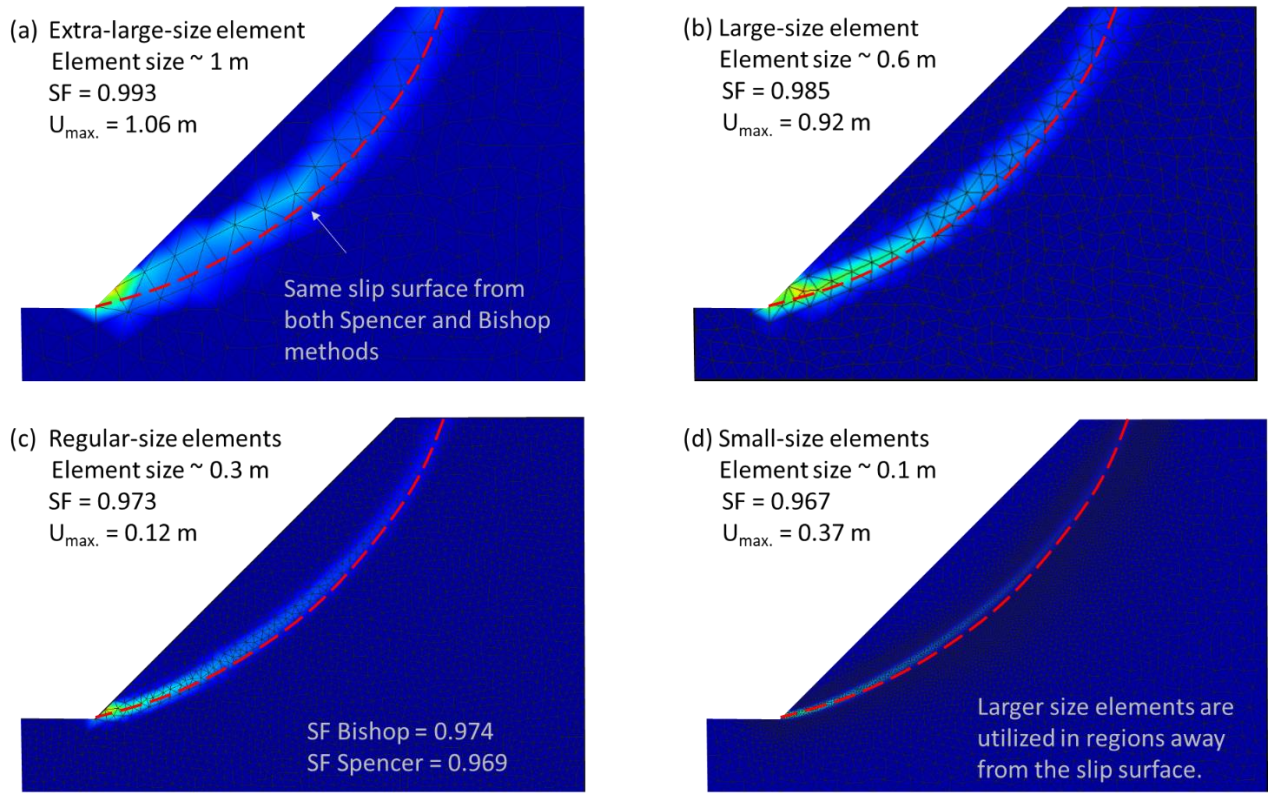

Fig. 4. Results from different element sizes (Model A)

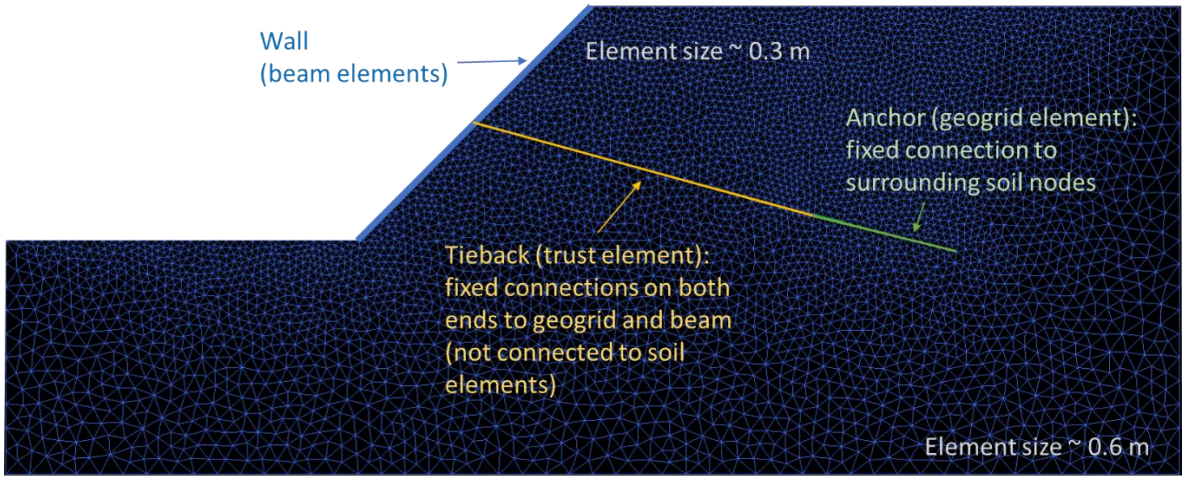

Fig. 5. Mesh plot of the slope with a single row of tiebacks

Stage 2 SRFEM analyses of the anchored slope from Model B contain 72 steps. The equivalent magnitudes of plastic strains from two of these 72 steps are presented in **Fig. 6**. There is no prestress in the tieback. **Fig. 6a** shows the resulting equivalent magnitude of plastic strain at a safety factor of 1.192. In this step, shear strength has been reduced by a factor of 1.192. Since the model slope without the tieback has a safety factor of less than 1.0 (~0.97), tension in the tieback is needed to maintain stability. The resulting tension calculated from EnFEM is 472 kN. Similarly, **Fig. 6b** shows the resulting equivalent magnitude of plastic strain at a safety factor of 1.604. In this step, the resulting tension is 1,554 kN. Applying tension values of 472 and 1,554 kN in EnSlope (a LEM program), the resulting safety factors from the Simplified Bishop method are 1.175 and 1.591, respectively, which are very close to those from SRFEM. It is interesting to note in **Fig. 6** that the volume of the sliding mass increases with decreasing soil strength as the safety factor increases.

Figure 7 shows the safety factors versus the resulting tension in the tieback from SRFEM. The calculated safety factors using both the Simplified Bishop method and Spencer's method are shown in the figure. Results from SRFEM using the non-associated flow rule (Model C) are also presented in **Fig. 7**. The difficulty associated with the non-associated flow rule reported by Tschuchnigg et al. (2015a) is again encountered in this study. The resulting tension of the last converged solution is 1,554 kN from Model B ($\psi = \phi'$) versus 1,261 kN from Model C ($\psi = 0$). However, converged results from both models are close to each other and are slightly higher than those from the Simplified Bishop method. The resulting safety factors from Spencer's method are generally lower than those from the Simplified Bishop method. It should be noted that the ultimate strength of a 1-inch (2.54 cm) steel bar is 567 kN. Data points with a tieback force greater than 567 kN have no physical meaning. However, these data points are shown in the figure to showcase how close the resulting safety factors from LEM and SRFEM are. For ease of discussion, the safety factor versus tieback force curve from the Simplified Bishop method is referred to as the Bishop curve hereafter.

Comparisons between safety factors are better presented by the difference between the two methods. As shown in **Fig. 8**, safety factors obtained from the SRFEM (Model B, $\psi = \phi'$) are only 0.004 to 0.021 higher than those from the Simplified Bishop method. The differences are comparable to the difference between Spencer's method and the Simplified Bishop method, which varies between -0.027 and +0.014. These differences are about 10 times smaller than those from slopes without tiebacks shown in **Fig. 3**. This is due to the differences in how safety factors are defined between an unreinforced slope and a tieback-reinforced slope. During the strength reduction stage of the SRFEM analyses, soil strengths reduce as safety factors increase in each incremental step. For an unreinforced slope, deformations increase until a converged solution is found in each step. Soil strengths are further reduced in the following step until the algorithm cannot converge. The safety factor associated with the last converged step or the safety factor associated with a given deformation is defined as the safety factor of the unreinforced slope. As discussed before, it can be difficult to determine the safety factor based on the last converged step. On the other hand, for a slope reinforced with tiebacks, both deformations and the tieback force increase as safety factors increase in each step. The resulting tieback force is the force required for stability at each given safety factor. This process is reversed in LEM, where the safety factor from a trial slip surface is calculated with a given tieback force. The good agreement between results from SRFEM and LEM shows that the Load Distribution Method provides good accuracy in determining safety factors for Model B.

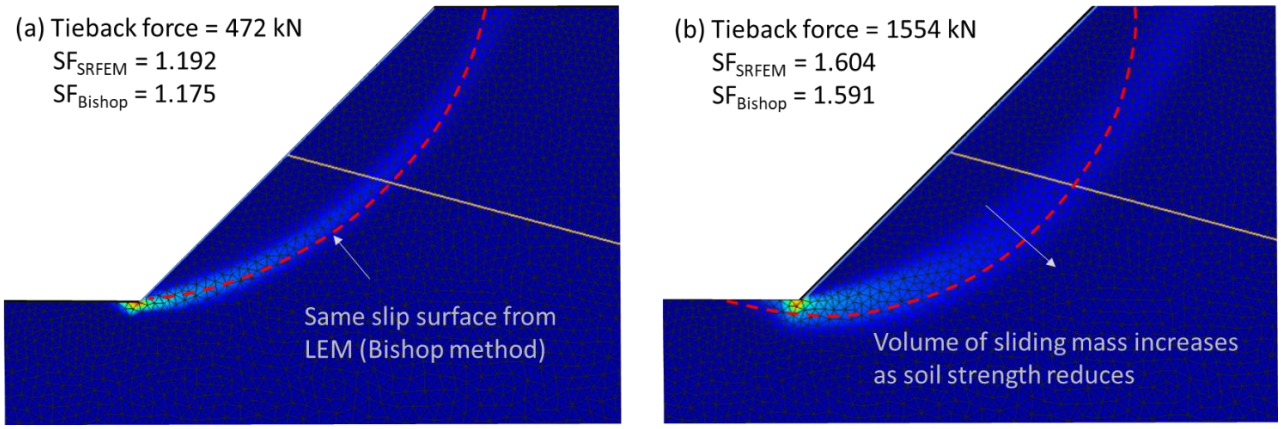

Fig. 6. Tieback force and SF from two different steps in Stage 2 SRFEM analyses (Model B)

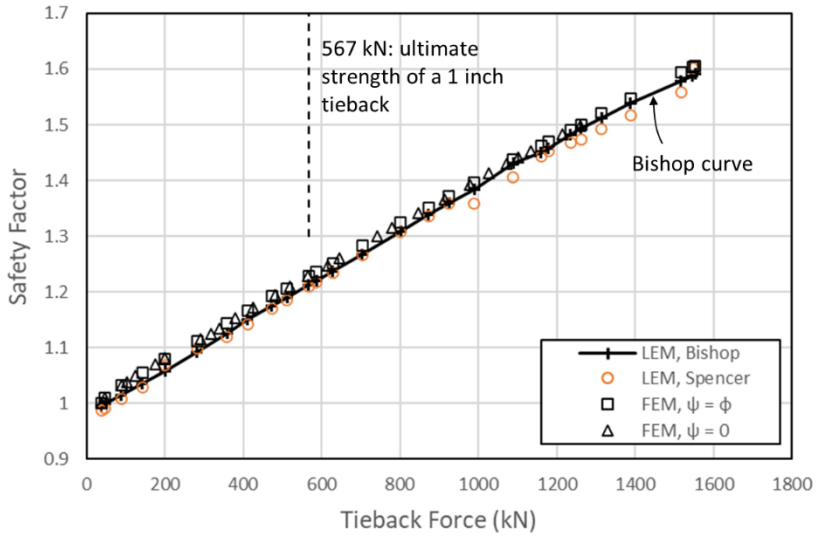

Fig. 7. Safety factors versus resulting tension from Model B

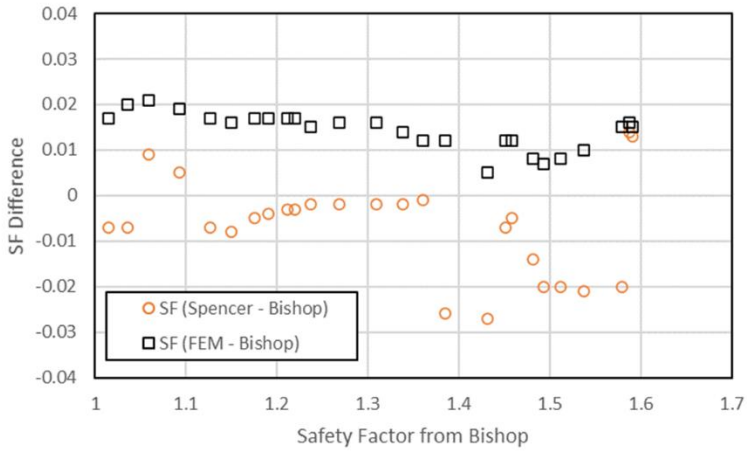

Fig. 8. Safety factor difference between LEM and SRFEM from Model B

Results from Models D and E are presented in **Fig. 9**. A prestress of 450 kN is added to the tieback in Model D, and soil stiffness is reduced to 10% from 10^5 kPa to 10^4 kPa in Model E. As shown in the figure, results from Model D are generally close to the Bishop curve, except those points circled in a red dashed line. In Model D, a prestress of 450 kN is applied during the first stage; hence, the tieback force at SF = 1 is 450 kN. As soil strength reduces with increasing safety factors, no additional force from the tieback is needed to maintain stability until the safety factor rises close to the Bishop curve. Once a slip surface is developed, the safety factor versus tieback force relationship follows the Bishop curve. **Fig. 10a** and **Fig. 10b** show the equivalent magnitude of plastic strain from the second step of stage 2 from Models B and D, respectively. As shown in the figure, a well-developed slip surface is shown in the result from Model B but not in that from

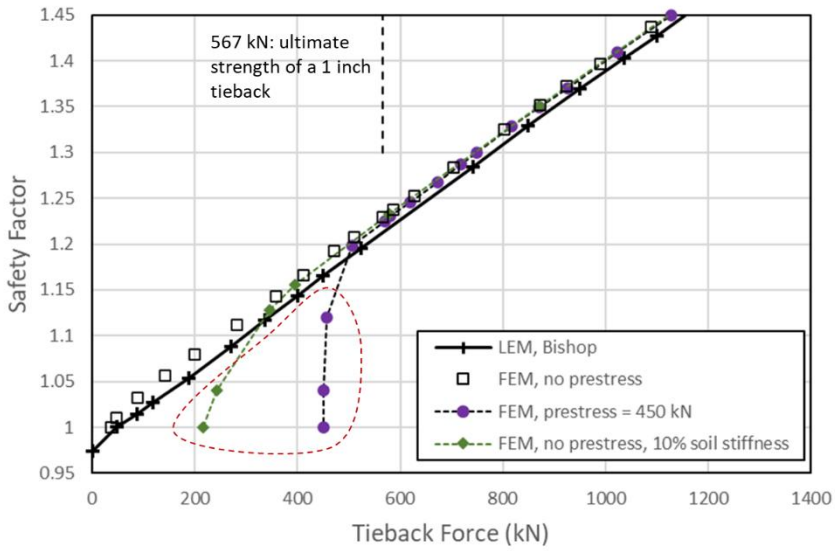

Fig. 9. Effects of prestress and soil stiffness

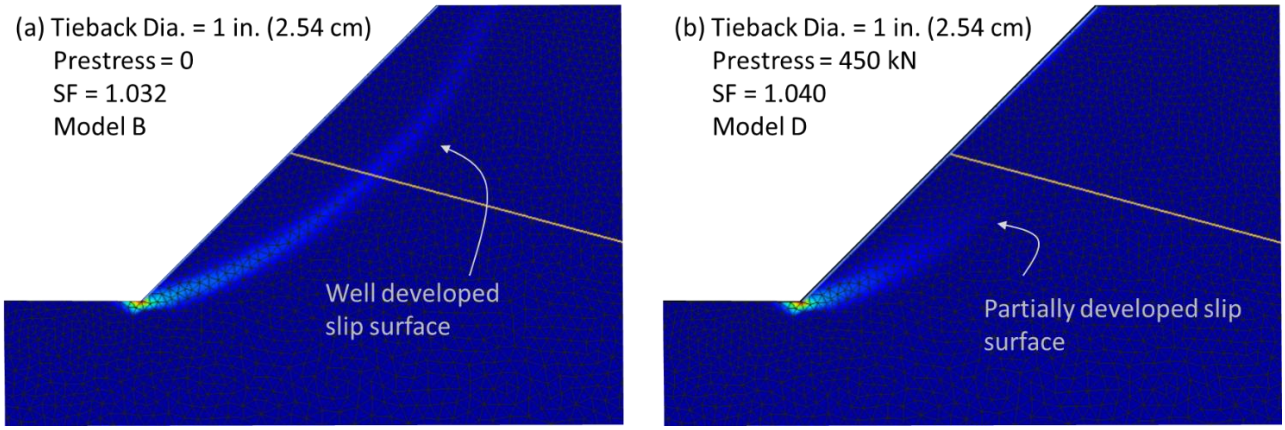

Fig. 10 Equivalent magnitude of plastic strain from the 2nd step of stage 2 from Models B and D

Model D. Similarly, due to the relatively lower stiffness of soil in Model E, there is a prestress incurred in the tiebacks during the first stage of the analyses. The resulting tieback force at SF = 1.0 in Model E is 216 kN versus 38 kN in Model B. As soil strength reduces, the SF versus tieback force relationship is close to the Bishop curve.

Results from Model F with a larger diameter tieback are shown in **Fig. 11**. Results from Model F are generally close to the Bishop curve. However, noticeable differences can be seen in the lower and upper regions of the curve. Similar to Model E, in the region of lower safety factor, there is a prestress incurred in the tieback during the first stage of the analysis. The resulting tieback force at SF = 1.0 is 153 kN. As soil strength reduces, the SF versus tieback force relationship is close to the Bishop curve. It is interesting to note that when SF increases above 1.790, the resulting tieback force decreases with increasing SF and deviates from the Bishop curve. **Fig. 12** shows the resulting equivalent magnitude of plastic strain at a safety factor of 1.801. As shown in the figure, a clear slip surface is formed between the soil and the wall elements. At this stage, the soil is sliding away from the wall structure as the wall is held relatively in place by the tiebacks. The assumption of the wall moving with the sliding soil mass made in the LEM does not agree with the findings from SRFEM. LEM can't consider the failure mechanism developed by soil-structure interactions.

The final converged step from the SRFEM is at SF = 1.801 and a tieback force of 2,172 kN. The ultimate strength of a 2.5-inch (6.35 cm) diameter steel bar is 3,457 kN. Applying the Load Distribution Method in the Simplified Bishop method, we can continue to calculate the safety factor for the tieback force up to 3,457 kN. However, as shown in **Fig. 11**, safety factors calculated from tieback forces greater than 2,200 kN using Simplified Bishop method may not be valid. It is interesting to note that using the Load Distribution Method, results from Spencer's method show converging issues for tieback forces greater than 2,000 kN. For example, at a tieback force of 2,200 kN, only 591 out of the 5,000 trial surfaces provide converged solutions. The number

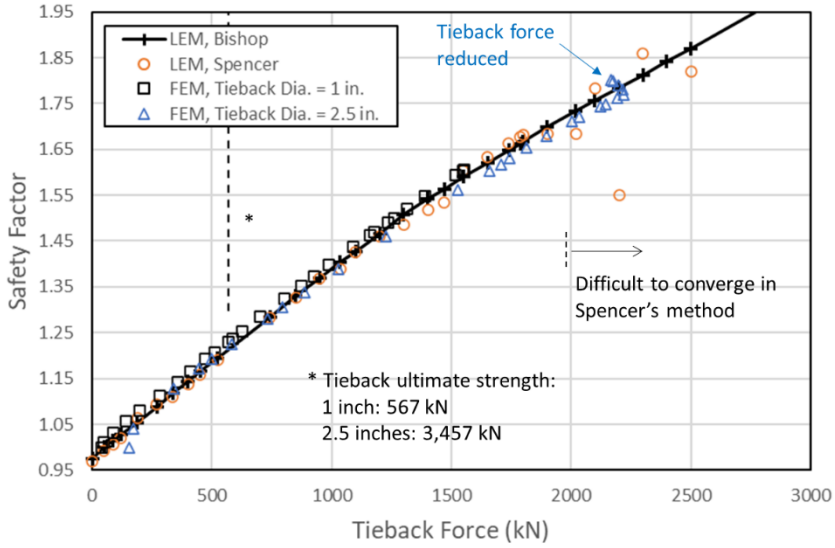

Fig. 11 Effects of the size of the tieback diameter

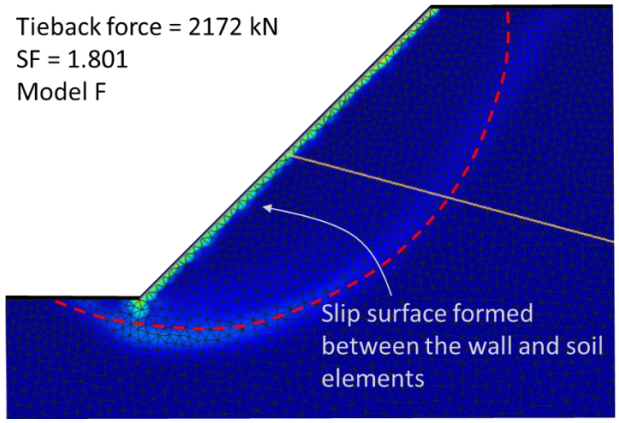

Fig. 12 Failure mechanism at the last converged step of the SRFEM

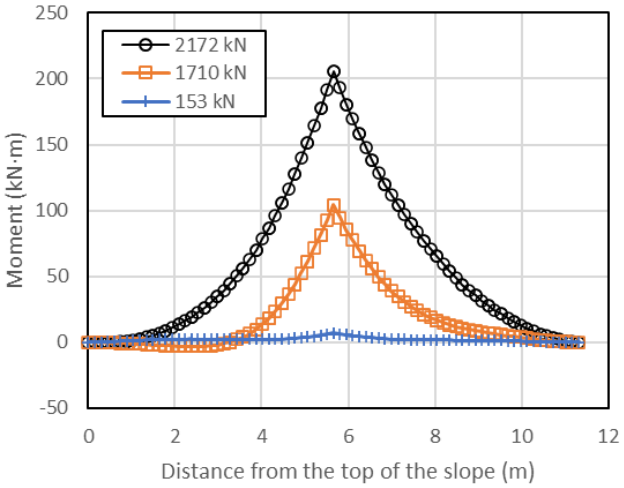

Fig. 13 Moment outputs from Model F

is down to 46 out of 5,000 at a tieback force of 2,400 kN. Although Spencer's method is more rigorous, it can have issues of convergence for some slip surfaces. In some cases, safety factors might not be considered for the most critical slip surface. It is a good engineering practice to verify results from Spencer's method with another slope stability analysis method.

Upon close inspection of **Fig. 11**, one will find the resulting safety factors from Model F are slightly lower than those from Model B in the range of safety factors between 1.05 and 1.6. This indicates that, at the given soil strength, a tieback with a larger diameter will carry more load than a tieback with a smaller diameter. This shows that the results of a tieback-reinforced slope are influenced by the sizes of the tiebacks. However, LEM can't consider the effect of tieback diameters.

In addition to the tieback force, SRFEM can also calculate the resulting moment and shear in the concrete facing wall. **Fig. 13** shows the moment outputs from 3 selected steps in Model F with a 2.5-inch (6.35 cm) diameter steel bar. The safety factors of the three steps are 1.0, 1.62, and 1.801. The corresponding tieback forces are 153kN, 1,710kN, and 2,172kN, respectively. As shown in the figure, the moment demands increase with increasing tieback forces. These outputs are needed for the structure designs of the tieback system.

CONCLUSIONS

This study utilized the Strength Reduction Finite Element Method (SRFEM) to examine the accuracy of the Load Distribution Method utilized in the Limit Equilibrium Method (LEM). Results from a hypothetical 45°

slope of a uniform soil layer show that safety factors obtained from SRFEM are generally close to those obtained from LEM when a slip surface is well developed in the soil mass. In these cases, the Load Distribution Method can provide a good approximation for analyzing a tieback-reinforced slope. However, LEM can't model soil-structure interactions, and LEM can't determine the maximum tieback force limited by the failure mechanism developed from soil-structure interactions. The findings from this study are summarized below.

1. Safety factors obtained from SRFEM are close to those obtained from LEM using the Load Distribution Method when a slip surface is well developed in the soil mass. The Load Distribution Method provides a good approximation for analyzing a tieback-reinforced slope in these cases.
2. Increasing the size of the tieback can have an influence on the resulting safety factor as more loads are carried by the tieback. The phenomenon can't be observed in LEM analyses.
3. SRFEM shows there is a limit to applying the tieback force. For a slope with a 2.5-inch (6.35 cm) diameter steel bar, a slip surface between the wall and the soil mass developed at a tieback force of around 2,200 kN. The assumption of the wall moving with the sliding soil mass made in LEM is not valid. The safety factor calculated from LEM with a tieback force higher than 2,200 kN may not be valid.
4. Although Spencer's method is more rigorous, it can have issues of convergence for some slip surfaces, and no safety factor can be obtained for those surfaces. As a result, the resulting safety factor might not include the most critical slip surface. It is a good engineering practice to verify results with multiple methods.
5. In addition to the tieback force, SRFEM can also calculate the moment and shear demands in the concrete facing wall, which are beneficial for structure designs.

It should be noted that these conclusions are based on a hypothetical slope of a single soil type. Additional studies are needed to verify the findings for slopes of different geometries and soil types.

REFERENCES

1. Burman, A., Acharya, S. P., Sahay, R. R., Maity, D., 2015. A comparative study of slope stability analysis using traditional limit equilibrium method and finite element method. Asin Journal of Civil Engineering Vol. 16-4, pp. 467-492.
2. Carpenter J. R., 1985. PCSTABL4 User Manual. Joint Highway Research Project JHRP-85-7, School of Civil Engineering, Purdue University, West Lafayette, In.
3. Carpenter, J. R., 2017. Analysis of Tieback Slopes and Walls Using STABL5 and PCSTABL5. Transportation Research Record.
4. Cheng, Y. M., Lansivaara, T., and Wei., W. B., 2007. Two-dimensional slope stability analysis by limit equilibrium and strength reduction methods. Comput. Geotech. 34 (3), pp.137–150.
5. Flamant A., 1886. Stabilite des constructions: resistance des materiaux. Paris, France.
6. Griffiths, D., Lane, P., 1999. Slope Stability Analysis by Finite Elements. Géotechnique 51, pp. 653–654.
7. Griffiths, D. V., and Marquez. R. M., 2007. Three-dimensional slope stability analysis by elasto-plastic finite elements. Géotechnique 57 (6), pp. 537–546.
8. Krabbenhoft K., Karim M.R., Lyamin A.V., Sloan S.W., 2012. Associated computational plasticity schemes for nonassociated frictional material. Int J Numer Method Eng, 90:1089–117.
9. Lee, D. H.; Cunningham, C. E.; Geraci, K. E.; Lee, D. E., 2010. Using Tieback Anchors to Stabilize an Active Landslide in San Juan Capistrano, California. In Earth Retention Conference 3. American Society of Civil Engineers: Bellevue, Washington, United States, pp. 910–919.
10. Nordal S., 2008. Can we trust numerical collapse load simulations using nonassociated flow rules? In: Singh, editor, Proceedings of 12th International Conference of the International Association of Computer Methods and Advances in Geomechanics (IACMAG), Goa, India, pp. 755–762.
11. Sabatini et al., 1999. FHWA-IF-99-15 Ground Anchors and Anchored Systems
12. Theinat, A., Salgado, R., Prezzi, M., Sakleshpur, V. A., 2024. Stability and Factor of Safety of Gravity-Retaining Structures Using the Strength Reduction Method. Journal of Geotechnical and Geoenvironmental Engineering, 150 (12), 04024118.
13. Tschuchnigg, F., Schweiger, F., Sloan, W., 2015. Slope Stability Analysis by Means of Finite Element Limit Analysis and Finite Element Strength Reduction Techniques. Part I: Numerical Studies Considering Non-Associated Plasticity. Computers and Geotechnics 70, 169–177.
14. Tschuchnigg, F., Schweiger, F., Sloan, W., 2015. Slope Stability Analysis by Means of Finite Element Limit Analysis and Finite Element Strength Reduction Techniques. Part II: Back Analyses of a Case History. Computers and Geotechnics 2015, 70, 178–189.